

Polar and nonpolar orderings in the electrically induced isotropic-nematic phase transition

Mingxia Gu,¹ Sergij V. Shiyankovskii,^{1,2} and Oleg D. Lavrentovich^{1,2,*}

¹Chemical Physics Interdisciplinary Program, Kent State University, Kent, Ohio 44242, USA

²Liquid Crystal Institute, Kent State University, Kent, Ohio 44242, USA

(Received 7 May 2008; published 9 October 2008)

We study the dynamics of the isotropic-nematic phase transition caused by an applied electric field at the time scales of dielectric relaxation. In the classic Landau-Khalatnikov theory of the phase transition dynamics, the nematic (nonpolar) order parameter is an instantaneous function of the applied field. We demonstrate that, when the field is changing faster than the time of dielectric relaxation, the induced polar order dynamics influences the dynamics of the nonpolar order parameter. We develop a model based on the Langevin equation to describe the simultaneous dynamics of both polar and nonpolar order parameters; the model is supported by experiment.

DOI: 10.1103/PhysRevE.78.040702

PACS number(s): 61.30.Gd, 64.70.M-, 77.22.Gm, 77.84.Nh

INTRODUCTION

The dynamics of phase transitions is a fundamental problem of statistical physics. It is usually described by the Landau-Khalatnikov (LK) theory, in which the order parameter evolution is determined by the corresponding free energy, which is a function of external parameters such as temperature, field, etc. In many cases, however, the external parameters influence the order parameter indirectly. A good example is the establishment of orientational nematic (N) order by an electric field \mathbf{E} . The N order is described by the Landau-de Gennes expansion with a nonpolar scalar order parameter S [1]:

$$f = f_0 + \frac{1}{2}a(T - T^*)S^2 - \frac{1}{3}bS^3 + \frac{1}{4}cS^4 + \dots - \frac{\epsilon_0 \Delta \epsilon_m}{3} E^2 S, \quad (1)$$

where f_0 is the free-energy density of an isotropic (I) phase with $S=0$; a , b , and c are the expansion coefficients; T and T^* are the actual and supercooling temperatures, respectively; and $\Delta \epsilon_m$ is the maximum dielectric anisotropy for $S=1$. However, the prime effect of \mathbf{E} is the establishment of *polar* order in the material, through a macroscopic electric polarization \mathbf{P} . This polarization \mathbf{P} depends on the dielectric tensor and therefore on the order parameter S ; as a result, the standard dielectric term $\frac{1}{2}\mathbf{P} \cdot \mathbf{E}$ leads to the last term in Eq. (1). The relationship between this term and dielectric anisotropy and their temperature dependence has been discussed in Ref. [2]. In this work, we discuss the role of \mathbf{P} in the dynamics of the field-induced isotropic-to-nematic phase transition. The relevant LK equation for this dynamics [3],

$$\gamma \frac{\partial S(t)}{\partial t} + \frac{\partial f}{\partial S} = 0 \quad (2)$$

(γ is the effective viscosity coefficient), considers the interaction between \mathbf{E} and S as a direct and instantaneous one; the evolution of \mathbf{P} that is ultimately responsible for the link between \mathbf{E} and S is completely ignored. The goal of this work is to determine the dynamics of both \mathbf{P} and S during the field-induced I-N phase transition. Theoretically, the problem

boils down to the derivation of dynamical equations for $\mathbf{P}(t)$ and $S(t)$ using the Langevin approach, while experimentally we measure $\mathbf{P}(t)$ and $S(t)$ in response to a polarity reversal of a strong electric field that establishes an N phase with both polar (\mathbf{P}) and nonpolar (S) order.

THEORY

Consider a uniaxial nematic liquid crystal (LC) with a director $\hat{\mathbf{n}}$ parallel to an applied electric field \mathbf{E} . Using the Maier-Saupe model, the orientational potential of a given molecule with a permanent dipole μ along the long axis can be expressed as the sum of Legendre polynomials $P_n(\cos \theta)$ [4,5]:

$$V(\theta) = -\mu E(t) P_1(\cos \theta) - [(\alpha_{\parallel} - \alpha_{\perp}) E^2(t) + B \bar{P}_2(t)] P_2(\cos \theta), \quad (3)$$

where θ is the angle between μ and $\hat{\mathbf{n}}$, α_{\parallel} and α_{\perp} are the molecular polarizabilities parallel and perpendicular to the long molecular axis, the overbar on $\bar{P}_2(t)$ and in what follows implies an ensemble average, and B is the parameter of the Maier-Saupe potential [4]. The Langevin equations for the dynamics of $\bar{P}_n(t)$ for this potential are [5]

$$\begin{aligned} \tau_n \frac{\partial \bar{P}_n(t)}{\partial t} = & - \left(1 - \frac{3}{(2n-1)(2n+3)} \right) \bar{P}_n(t) \\ & + \frac{e(t)}{2n+1} [\bar{P}_{n-1}(t) - \bar{P}_{n+1}(t)] \\ & + \frac{3u(t)}{2n+1} \left(\frac{n-1}{2n-1} \bar{P}_{n-2}(t) - \frac{n}{2n+3} \bar{P}_{n+2}(t) \right), \end{aligned} \quad (4)$$

where $\tau_n = 2\tau/n(n+1)$ is the rotational relaxation time for $\bar{P}_n(t)$ in the I state, τ is the Debye relaxation time in the I phase, $u(t) = [\xi e^2(t) + B \bar{P}_n(t)]/k_B T$, $\xi = k_B T(\alpha_{\parallel} - \alpha_{\perp})/3v\mu^2$, and $e(t) = \mu E(t)/k_B T$ is the normalized electric field, k_B is the Boltzmann constant, and v is the volume per molecule. Note that the parity of n defines the parity of $\bar{P}_n(t)$ with respect to $e(t)$.

In Eq. (4), the slowest relaxation should be observed for $\bar{P}_1(t)$ and $\bar{P}_2(t)$ since $\tau_n \propto n^{-2}$ and since the relaxation of

*odl@lci.kent.edu

these quantities is hindered by specific slow-down effects such as an energetic barrier for flip-flop of permanent dipoles and the proximity of the N-I phase transition, respectively. Thus we can assume that the higher-order polynomials with $n \geq 3$ reach the equilibrium state instantaneously. Their equilibrium values can be found as stationary solutions of Eq. (4) for $n \geq 3$ controlled by the current values of $\bar{P}_1(t)$ and $\bar{P}_2(t)$. Using these solutions for $\bar{P}_3(t)$ and $\bar{P}_4(t)$, we obtain the close set of dynamic equations for $\bar{P}_1(t)$ and $\bar{P}_2(t)$:

$$\tau \frac{\partial \bar{P}_1(t)}{\partial t} = \frac{e(t)}{3} - M_{11}(t)\bar{P}_1(t) + M_{12}(t)e(t)\bar{P}_2(t), \quad (5)$$

$$\tau \frac{\partial \bar{P}_2(t)}{\partial t} = \frac{3u(t)}{5} + M_{21}(t)e(t)\bar{P}_1(t) - M_{22}(t)\bar{P}_2(t), \quad (6)$$

where $M_{jk}(t) > 0$ are functions of $\bar{P}_2(t)$ and $e^2(t)$. Equations (5) and (6) describe the dynamics of the polarization $P(t) = \mu \bar{P}_1(t)/v$ and the order parameter $S(t) = \bar{P}_2(t)$ of the uniaxial N system under the electric field $e(t)$.

Considering $e(t)$ as an independent function, we obtain a general solution for Eq. (5):

$$\bar{P}_1(t) = \bar{P}_1^{\text{ins}}(t) + \bar{P}_1^{\text{mem}}(t), \quad (7)$$

$$\bar{P}_1^{\text{ins}}(t) = \frac{1 + 3M_{12}(t)\bar{P}_2(t)}{3M_{11}(t)}e(t),$$

$$\begin{aligned} \bar{P}_1^{\text{mem}}(t) &= \bar{P}_{10}F(t) - \bar{P}_1^{\text{ins}}(t) \\ &+ \frac{F(t)}{\tau} \int_0^t \frac{e(t')}{F(t')} \left(\frac{1}{3} + M_{12}(t')\bar{P}_2(t') \right) dt', \end{aligned}$$

where $\bar{P}_1^{\text{ins}}(t)$ is the instantaneous response (equivalent to the one used in the LK model), and $\bar{P}_1^{\text{mem}}(t)$ is a memory term that is caused by the finite relaxation of the polarization and disappears when $\tau \rightarrow 0$; here $F(t) = \exp[-(1/\tau) \int_0^t M_{11}(t') dt']$. Substituting the solution (7) into (6), we obtain the dynamical equation for $\bar{P}_2(t)$:

$$\begin{aligned} \tau \frac{\partial \bar{P}_2(t)}{\partial t} &= \frac{3u(t)}{5} - M_{22}(t)\bar{P}_2(t) + \frac{1 + 3M_{12}(t)\bar{P}_2(t)}{3M_{11}(t)}M_{21}(t)e^2(t) \\ &+ M_{21}(t)e(t)\bar{P}_1^{\text{mem}}(t), \end{aligned} \quad (8)$$

where the first three terms on the right-hand side are equivalent to the LK model, whereas the last term represents the effect of the finite rate of polarization relaxation. We turn now to the experimental determination of $\bar{P}_1(t) = vP(t)/\mu$ and $\bar{P}_2(t) = S(t)$.

EXPERIMENT

A cell of the classic sandwich type was constructed with a reduced area of the indium tin oxide (ITO) electrodes, $A = 5 \text{ mm}^2$, separated by a gap $d = 3.8 \text{ }\mu\text{m}$. The purpose of using a small active area is to reduce the RC load, and thus to reduce the delay of the electric field applied to the LCs [6].

No polyimide alignment layer is used to avoid the drop of potential across such a layer [7]. The cell is stabilized in an LTS120 hot stage (Linkam Scientific Instruments), with an accuracy of 0.1 K. We use a pulse generator HV1000 (Direct Energy) capable of changing the voltage within a few tens of nanoseconds. We chose *p*-cyanophenyl *p*-*n*-heptylbenzoate (CP7B), $T_C = 330 \text{ K}$, $v = 2.86 \times 10^{-28} \text{ mm}^3$, as the nematic LC, because of its large longitudinal moment ($\mu = 5.6 \text{ D}$ [8]) and relatively long dielectric relaxation time (tens of nanoseconds in the I phase).

The LC, kept at $T > T_C$, was subject to a strong electric voltage that abruptly changed its polarity. We first applied $U_0 = 100 \text{ V}$ to establish the field-induced polar $\bar{P}_{10}(T, U_0)$ and nonpolar $\bar{P}_{20}(T, U_0)$ order parameters. The time duration of the pulse was 1.5 ms, long enough to accumulate all ions near the substrates and to saturate both \bar{P}_{10} and \bar{P}_{20} , as evidenced by the decrease of electric current down to 0 and by saturated light transmittance through the cell. Note that the applied voltage is well above the typical ‘‘anchoring breaking’’ threshold [9], so that the ordered state can be considered uniformly homeotropic throughout the cell.

At time $t=0$, the polarity of the field was reversed abruptly, within $\sim 100 \text{ ns}$. The sharp voltage reversal was essential to trace the dynamics of both $\bar{P}_1(t)$ and $\bar{P}_2(t)$. The sharp polarity reversal should flip the direction of \mathbf{P} . If $\bar{P}_1(t)$ adjusts instantaneously to the field reversal, then $\bar{P}_2(t) = \text{const}$ during the instantaneous polarity reversal, as it depends on $e^2(t)$. Our experiments below demonstrate that $\bar{P}_2(t)$ does change; these changes can be attributed not only to the finite rate of voltage change but also to the finite rate of $\bar{P}_1(t)$ adjustment caused by the finite rate of Debye dielectric relaxation.

There are two thermal effects associated with the applied voltage. First, as established by Lelidis and Durand [10], the field-induced orientational order is accompanied by an adiabatic temperature increase ($< 0.5 \text{ K}$) within the first $1 \text{ }\mu\text{s}$, which then relaxes over the period of time $\sim 100 \text{ }\mu\text{s}$. Since the voltage reversal in our experiments was performed 1.5 ms after the voltage switch-on, this adiabatic temperature variation has already decayed. Furthermore, our experiment was designed to eliminate the very cause for the Lelidis-Durand thermal effect: since the voltage amplitude remains the same, the stationary values of the field-induced $\bar{P}_2(t)$ before and after the voltage reversal should be the same ($= \bar{P}_{20}$). The second thermal effect comes from the dielectric heating caused by reorientation of $\bar{P}_1(t)$. An upper limit of the temperature change can be estimated as $\sim T\bar{P}_{10}^2$ which is $\sim 1 \text{ K}$. As shown below, this heating leads to small changes in the stationary value of $\bar{P}_2(t)$ established after the voltage reversal.

To determine the polarization $P(t)$, we used the Martinot-Lagarde method [11] by serially connecting the cell with a resistor $R = 50 \text{ }\Omega$ and the generator. Under this measurement scheme,

$$P(t) = P_0 - \varepsilon_0 \varepsilon_{\parallel}^h(T, e_0) \frac{U_{\text{LC}}(t) - U_0}{d} - \frac{1}{A} \int_0^t \frac{U_R(t')}{R} dt', \quad (9)$$

where $P_0 = \varepsilon_0 [\varepsilon_{\parallel}^l(T, e_0) - \varepsilon_{\parallel}^h(T, e_0)] U_0 / d$, $U_R(t)$ is the voltage drop at $R = 50 \text{ }\Omega$, $U_{\text{LC}}(t) = U(t) - U_R(t)(1 + R_{\text{ITO}}/R)$ is the volt-

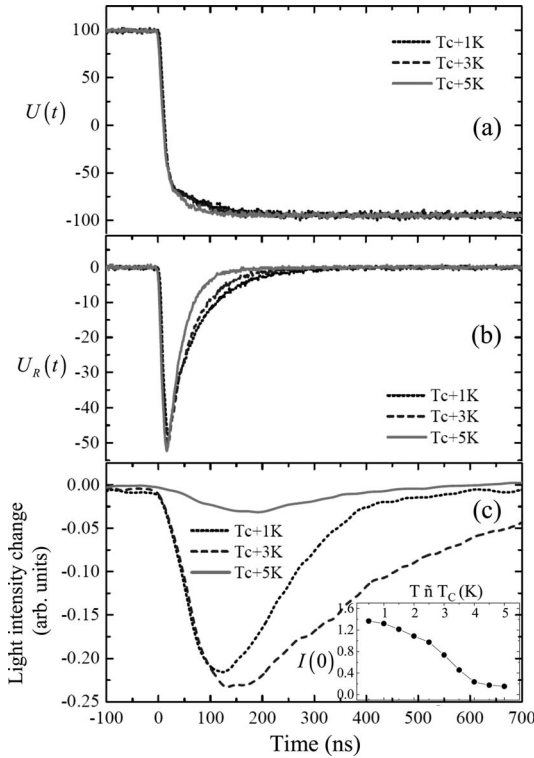


FIG. 1. Experimental data of (a) total voltage $U(t)$, (b) voltage drop $U_R(t)$ on the resistor R , and (c) transmitted light intensity change $I(t)-I(0)$ with respect to the stationary value $I(0)$ [inset of (c)] at different temperatures.

age across the LC, $R_{ITO}=80 \Omega$; $U_{LC}(t \leq 0)=U_0$; and $\varepsilon_{\parallel}^l(T, e_0)$ and $\varepsilon_{\parallel}^h(T, e_0)$ are the values of the parallel component of the dielectric tensor at low and high frequencies. To trace $P(t)$, one needs to know all the parameters on the right-hand side of Eq. (9). $U(t)$ and $U_R(t)$ are measured directly, Figs. 1(a) and 1(b). Their dynamics is temperature dependent. The small temperature dependence of $U(t)$ is related to the changes in the load caused by the temperature-sensitive behavior of the LC cell. The temperature dependence of $U_R(t)$ is much more pronounced because it is related directly to the temperature sensitivity of the field-induced polar order dynamics and cannot be simply explained by the temperature change $\Delta\varepsilon_{\parallel}^l(T, e_0)$, because $\Delta\tau_{RC}=(R_{ITO}+R)\varepsilon_0\Delta\varepsilon_{\parallel}^l(T, e_0)A/d < 5$ ns; see the estimates below.

The rest of the parameters in Eq. (9) were evaluated as follows. We have found that $\varepsilon_{\parallel}^h(T, e_0)$ can be considered as a constant for CP7B in the range of the interest. At zero field and $T=T_C-7$ K, $\varepsilon_{\parallel}^h(T, 0)$ was determined to be 4.0 by fitting the dielectric relaxation spectrum with the Debye model. In the I phase, $T=T_C+1$ K, the Debye fit yields $\varepsilon_{\text{iso}}^h(T, 0)=4.2$. Since the two values are close, we consider $\varepsilon_{\parallel}^h(T, e_0)=4.1$ as independent of the temperature and of the field-induced order parameter (within the range of the existence of the field-induced N phase).

To determine $\varepsilon_{\parallel}^l(T, e_0)$ in the induced N phase, we use the experimental data on birefringence $\Delta n(T, e_0)$, as both quantities are related to the field-induced nonpolar order $S(T, e_0)$. Both $\Delta n(T, e_0)$ and $\varepsilon_{\parallel}^l(T, e_0)$ depend linearly on $S(T, e_0)$ [12] and are therefore linearly related, $\varepsilon_{\parallel}^l(T, e_0)=\varepsilon_{\text{iso}}^l + \eta\Delta n(T, e_0)$; here $\varepsilon_{\text{iso}}^l$ is the low-frequency dielectric constant in the I

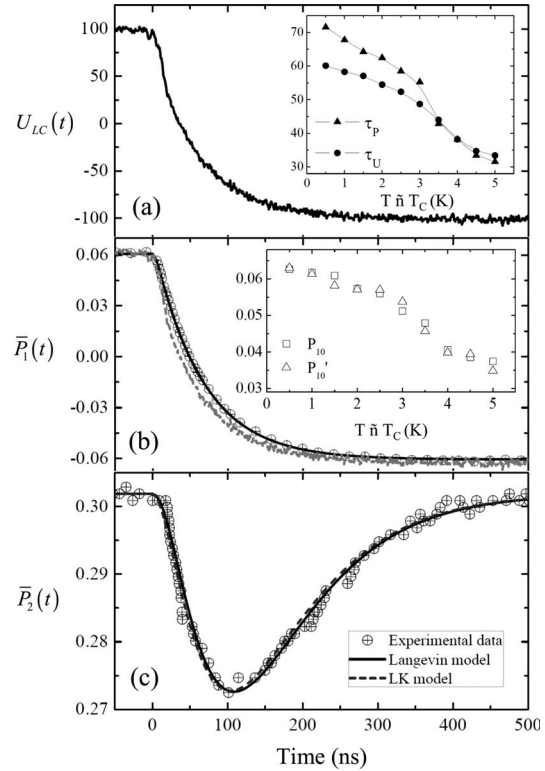


FIG. 2. Dynamics of (b) $\bar{P}_1(t)$ and (c) $\bar{P}_2(t)$ under (a) voltage polarity reversal ($t=0$) at $T=T_C+1$ K. In (b) and (c), the circles are experimental data and the solid and dashed curves are simulations. The insets in (a) and (b) are a comparison between τ_U and τ_P , between $\bar{P}_1(t)$ values before (\bar{P}_{10}) and after (\bar{P}'_{10}) polarity reversal at different temperatures. The dashed curve in (b) is the instantaneous response of $\bar{P}_1(t)$ under the polarity reversal.

phase, measured by us to be 16, and η is a fitting coefficient. We first measure $\varepsilon_{\parallel}^l(T, 0)$ and $\Delta n(T, 0)$ at zero field in the N phase within the range $[T_C-12 \text{ K}, T_C-1 \text{ K}]$ and fit the measured data to obtain $\eta=64 \pm 3$. This value allows us to calculate $\varepsilon_{\parallel}^l(T, e_0)$ in the induced N phase from $\Delta n(T, e_0)$.

Both $\Delta n(T, e_0)$ and $S(t)=\bar{P}_2(t)$ are determined in the same birefringence experiment as proposed by Lelidis *et al.* [13]. We measure the transmission of a He-Ne laser beam through a cell of known thickness and a pair of linear polarizers with photodetector TIA-500S-TS (Terahertz Technologies, Inc.), with response time $\tau_d < 1$ ns, which is much smaller than the measured times. We use oblique beam incidence and adjust the angle between the incident plane and the transmission axis of the polarizers to be 45.5° instead of 45° , to compensate for the reflectivity difference for s and p polarizations. $\Delta n(T, e_0)$ was obtained from the stationary transmitted intensity while $\bar{P}_2(t)$ was determined from the dynamics of the optical signal in response to the polarity reversal [Fig. 1(c)].

Figure 2 shows the dynamics of the voltage $U_{LC}(t)$ acting on the LC layer (a), and the polar $\bar{P}_1(t)$ (b) and nonpolar $\bar{P}_2(t)$ (c) order parameters caused by the polarity reversal. The voltage change $U_{LC}(t)$ is determined by the rate of the generator voltage reversal and by the transient effects in the LC “capacitor” that involve the high-frequency dielectric constant $\varepsilon_{\parallel}^h$ and the dynamics of polarization $P(t)$. In our

experiment, $U_{LC}(t)$ is fitted well with an exponential function,

$$U_{LC}(t) = U_0(2e^{-t/\tau_U} - 1), \quad (10)$$

where the characteristic time τ_U is in the range of 60–30 ns, decreasing with temperature as shown in the inset in Fig. 2(a). The polar order dynamics can also be fitted with the same functional dependence, $\bar{P}_1(t) = \bar{P}_{10}(2e^{-t/\tau_P} - 1)$, $\bar{P}_{10} = vP_0/\mu$, although the time constant τ_P is generally larger than τ_U [Fig. 2(a) inset]. One would observe $\tau_P = \tau_U$ if $\bar{P}_1(t)$ followed the changing electric field instantaneously; this regime is approached only at high temperatures $T > T_C + 3$ K. At lower temperatures $T \leq T_C + 3$ K, one clearly observes that $\tau_P > \tau_U$, reflecting the finite rate of dielectric relaxation. Note that the field reversal preserves the absolute value of the field-induced polar order \bar{P}_{10} , as evidenced by our experiments for ten temperature points [see inset in Fig. 2(b)]; this observation justifies our calculations based on Eq. (9).

The nonpolar order parameter $\bar{P}_2(t)$ does not remain constant during the polarity reversal, experiencing a temporary decrease by about 10% and then restoring its equilibrium value as $e(t) \rightarrow -e_0$. The smallness of experimentally observed changes in $\bar{P}_2(t)$ allows us to simplify the dynamic equations for the problem: in Eq. (7), $\bar{P}_2(t)$ and $M_{ij}(t)$ can be considered as time-independent constants \bar{P}_{20} and M_{ij0} , respectively, whereas Eq. (8) for the dynamics of $\bar{P}_2(t)$ can be linearized with respect to $\Delta\bar{P}_2(t) = \bar{P}_2(t) - \bar{P}_{20}$.

With the approximations above, using the exponential fit of $U_{LC}(t)$, Eq. (10), we find the solution (7) as

$$\bar{P}_1(t) = \bar{P}_{10} \left((2e^{-t/\tau_U} - 1) + \frac{2(e^{-t/\tau_U} - e^{-t/\tau_{nem}})}{\tau_U/\tau_{nem} - 1} \right). \quad (11)$$

The first term on the right-hand side of Eq. (11) describes an instantaneous contribution to $\bar{P}_1(t)$ (see above), while the second term is related to the finite rate of dielectric relaxation with the characteristic time $\tau_{nem} = \tau/M_{11}$. The solution (11) with τ_{nem} in the range 10–30 ns fits the experiment closely, somewhat better than the model based on an instantaneous dielectric response.

To analyze $\bar{P}_2(t)$, we linearize Eq. (8) with respect to $\Delta\bar{P}_2(t)$ and $e^2(t) - e_0^2$ [note that the time interval during which $e^2(t) \neq e_0^2$ is rather short, ~ 150 ns] and use solution (11) for $\bar{P}_1(t)$ and $e(t) = e_0(2e^{-t/\tau_U} - 1)$, to arrive at the analytical solution for $\Delta\bar{P}_2(t)$:

$$\Delta\bar{P}_2(t) = \frac{h}{\tau_S} \exp\left(-\frac{t}{\tau_S}\right) \int_0^t H(t') \exp\left(\frac{t'}{\tau_S}\right) dt', \quad (12)$$

where τ_S is the characteristic time for $\Delta\bar{P}_2(t)$ and h is the measure of its amplitude; the last term in $H(t) = (2e^{-t/\tau_U} - 1)^2 + 2(e^{-t/\tau_U} - e^{-t/\tau_{nem}})(2e^{-t/\tau_U} - 1)/(\tau_U/\tau_{nem} - 1)$ represents the dielectric memory contribution. The integral (12) is analytical but the final expression is too cumbersome to be presented explicitly. Equation (12) provides a good fit of the experimental data in Fig. 2(c) with $\tau_S = 95$ ns and $h = 0.058$. The same experiment can also be fitted with the LK model, neglecting the last term in Eq. (12), and using $\tau_S = 95$ ns, $h = 0.060$. In the LK approach, as seen by comparing Eq. (12) to Eqs. (1) and (2), $\tau_S = \gamma/[\partial f/\partial S]_{e=e_0}$ and $h = \varepsilon_0 \Delta\varepsilon_m \tau_S U_0^2 / 3\gamma d^2$; note that, in our experiment, the order parameters change within a time interval that is much shorter than the characteristic time of thermal relaxation, so that $\partial f/\partial S$ should be evaluated for an adiabatic regime. The fact that both models fit the data well with the same $\tau_S = 95$ ns can be explained by the fact that, after $U_{LC}(t)$ and $\bar{P}_1(t)$ have relaxed to their new equilibrium values at $t \geq 250$ ns, $H(t)$ in Eq. (12) becomes close to zero and the corresponding integral approaches a constant value. In other words, $\Delta\bar{P}_2(t) \propto \exp(-t/\tau_S)$ at $t \geq 250$ ns. Since $\tau_S = \gamma/[\partial f/\partial S]_{e=e_0}$, this feature explains why the dynamics of $\bar{P}_2(t)$ observed at different temperatures is characterized by very different relaxation times, Fig. 1(c).

CONCLUSION

We have determined experimentally and theoretically the dynamics of both the polar and the nonpolar order parameters during an electric-field-induced I-N phase transition. In materials with polar molecules, the electric field induces the nematic nonpolar order indirectly, through its coupling to the polar order parameter. Note that in this work we consider the simplest possible geometry, with the molecular dipoles being parallel to the long axis of rodlike molecules and thus parallel to the field-induced director. In more complex geometries, for example, when the molecular dipoles are perpendicular to the long molecular axis, the coupling of polar and nonpolar order parameters should lead to a much broader variety of the induced order, including a possible formation of biaxial phases and phases with a negative $S = \bar{P}_2(t)$.

The work was supported by DOE Grant No. DE-FG02-06ER 46331.

[1] P. G. de Gennes and J. Prost, *The Physics of Liquid Crystals* (Clarendon, Oxford, 1993).
 [2] G. Basappa and N. V. Madhusudana, *Eur. Phys. J. B* **1**, 179 (1998).
 [3] I. Lelidis and G. Durand, *Phys. Rev. Lett.* **73**, 672 (1994).
 [4] W. Maier and A. Saupe, *Z. Naturforsch. A* **14**, 882 (1959).
 [5] W. T. Coffey, Yu. P. Kalmykov, and J. T. Waldron, *The Langevin Equation*, 2nd ed. (World Scientific, Singapore, 2004).
 [6] H. Takahashi, J. E. Maclennan, and N. A. Clark, *Jpn. J. Appl. Phys.*, Part 1 **37**, 2587 (1998).

[7] R. N. Thurston, *J. Appl. Phys.* **55**, 3846 (1984).
 [8] G. W. Gray and S. M. Kelly, *J. Mater. Chem.* **9**, 2037 (1999).
 [9] I. Dozov and Ph. Martinot-Lagarde, *Phys. Rev. E* **58**, 7442 (1998).
 [10] I. Lelidis and G. Durand, *Phys. Rev. Lett.* **76**, 1868 (1996).
 [11] Ph. Martinot-Lagarde, *J. Phys. (France) Lett.* **38**, L17 (1977).
 [12] W. H. de Jeu, *Physical Properties of Liquid Crystalline Materials* (Gordon and Breach, New York, 1980).
 [13] I. Lelidis, M. Nobili, and G. Durand, *Phys. Rev. E* **48**, 3818 (1993).